Materials Science & Engineering C 117 (2020) 111293

Contents lists available at ScienceDirect

Materials Science & Engineering C

journal homepage: www.elsevier.com/locate/msec

Label-free detection of DNA by a dielectric modulated armchair-graphene nanoribbon FET based biosensor in a dual-nanogap setup

Mohammad K. Anvarifard[a], Zeinab Ramezani[b], Iraj Sadegh Amiri[c,d,*]

[a] Department of Engineering Sciences, Faculty of Technology and Engineering, East of Guilan, University of Guilan, Rudsar-Vajargah, Iran
[b] Department of Electrical and Computer Engineering, Northeastern University, Boston, MA 02115, USA
[c] Computational Optics Research Group, Advanced Institute of Materials Science, Ton Duc Thang University, Ho Chi Minh City, Viet Nam
[d] Faculty of Applied Sciences, Ton Duc Thang University, Ho Chi Minh City, Viet Nam

ARTICLE INFO

Keywords:
Armchair-graphene nanoribbon
DG-AGNRFET biosensor
DNA detection
Non-equilibrium green function

ABSTRACT

A Double-Gate Armchair-Graphene Nanoribbon FET is proposed to realize a high-sensitive and small-size biosensor in order to detect DNA without high-cost and time-consuming labeling process. Two nanogap cavities open inside the top and bottom gate oxides by the method of sacrificed layer etching. When the DNA biomolecule is introduced to the nanogap cavity, the hybridization event which is actually the formation of a double-strand of DNA will occur thus electrically modulating the GNR channel leading to a change in the drain current. The important report of this research is about attained high sensitivity of the proposed biosensor for a vast spectrum of the DNA biological samples. It is worth noting that a DNA sequence by 23 nucleotides extracted from *Neisseria gonorrhoeae* can be detected as a special case. An extensive numerical approach has been applied in order to characterize the proposed biosensor. The suggested biosensor has been evaluated by solving Schrödinger equation)SE(with Non-Equilibrium Green Function (NEGF) method in the mode-space coupled into Poisson solver in a self-consistent manner assuming ballistic limit. Two different expressions of sensitivity in terms of the threshold voltage and current have been defined giving a good metric for the sensitivity analysis. The results revealed a relative sensitivity of 1 mV/nm^2 by a filled area by the DNA about 120 nm^2 showing the excellent superiority for the proposed biosensor as compared to other counterparts. The effective area of the proposed biosensor obtains 240 nm^2 which is very small in comparison with other reports highlighting high capability of the biosensor in the detection. It has been shown that the proposed biosensor can be implemented in ultra-scaling domain resulting in considerable increase in the sensitivity promising a potent and reliable candidate for high-sensitive and small-size biosensors. Also, the technical issues on designing the suggested biosensor have been investigated to achieve a useful guideline in detection and identification of the target DNAs.

1. Introduction

A special biomolecule named as Deoxyribonucleic Acid (DNA) is very important and vital in modern medicine. It gives a powerful impulse to researchers in many fields having a direct and indirect dependence on human health [1–3]. There are many diseases detected by the DNA analysis and it is to note that this procedure is fast growing with an aggressive high slope [4].

Regarding very high importance for the DNA detection, different approaches in terms of fluorescent, electrochemical, enzymatic and magnetic have been proposed and provided to sense the DNA biomolecule hybridization [5–11]. Despite the advantageous of these methods, they suffer from low sensitivity and also labeling processes which are very costly and time-consuming steps [12] . Therefore, the efforts were done is to look for label-free approaches. The Ion-Sensitive Field-Effect Transistor (ISFET) concept has been considered as a good alternative to detect the DNA without the labeling procedure [13]. Moreover, there are big obstacles to use these biosensors because they need a buffer solution and do not qualify to extract the neutral DNAs [13].

Abbreviations: EP, electrical performance; DN, dual nanogap; PS, Poisson solver; DC, dielectric constant; SE, Schrödinger equation; DG, double gate; SCE, short channel effect; NC, nanogap cavity; BS, biosensor sensitivity; TVBS, Threshold Voltage Biosensor Sensitivity; DCBS, Drain Current Biosensor Sensitivity; RGF, Retarded Green Function; CBE, conduction band energy; NEGF, non-equilibrium green function; SA, sensitivity analysis; DM, dielectrically modulated; SAM, self-assembly monolayer; pDNA, probe DNA; tDNA, target DNA; RS, real space; MS, mode space; RLDOS, Resolved Local Density of Sates; SBP, silica-binding proteins

* Corresponding author at: Ton Duc Thang University, Ho Chi Minh City, Viet Nam.
E-mail addresses: m.anvarifard@guilan.ac.ir (M.K. Anvarifard), irajsadeghamiri@tdtu.edu.vn (I.S. Amiri).

https://doi.org/10.1016/j.msec.2020.111293
Received 23 February 2020; Received in revised form 1 July 2020; Accepted 14 July 2020
Available online 24 July 2020
0928-4931/

It is worth noting that impulses to fundamental research on the different semiconductor devices are so much that there are many works studying on the electrical performance (EP) improvement [14–21]. Owing to compatibility with CMOS technology, these devices are suitable for the aims of bio-sensing. To dominate the critical problems of ISFET, Dielectric-Modulated FET (DM-FET) structure has been introduced to detect the DNA hybridization without any labeling process and the buffet solution [22–24]. Since it only depends on the biosensor channel electrostatic, then both the charged and neutral DNAs will be successfully detected.

Regarding the dielectrically modulated (DM) concept-based structures, most of them are realized by the silicon material which are completely compatible with the CMOS technology. Moreover, all the efforts have been performing on scaling down these devices in order to reach high speed and the EP enhancement. But, the end of the roadmap of the semiconductor devices based on typical materials such as silicon is coming soon. Indeed, the short channel effects (SCEs) will be exhibited for the short channel lengths resulting in the degradation of the EP. That is why the attempts are mostly highlighted on the implementation of devices based on the new materials.

For example, graphitic carbon nitride (CN) has given a much interest as an emerging nitrogen-rich 2D carbon material in the applications in terms of photo-/electrocatalysts to biosensors. A report about conjunction with a π-π stacking interaction showed that bulk CN could be simultaneously exfoliated via facile mechanical grinding [25]. m-CNNS is successfully linked to a DNA probe, and the results showed much enhanced sensitivity.

One of other important new materials is called graphene. It is made by the carbon atom in a honeycomb lattice structure formation. In order to prepare it to be as a device it will be cut along the transport direction thus producing a very narrow thickness device named GNRFET. The superior EP of the GNRFET as compared to its traditional counterparts causes the wide spectrum of the research is attributed to it, nowadays [26–30]. It is worth noting that benefiting from the GNRFET as a biosensor has been neglected at most of the works. It is the first time that the paper introduces a double-gate (DG) armchair GNRFET biosensor by a dual-nanogap (DN) set up to get rid of the fundamental obstacles exhibited for the silicon DM-FETs.

In this paper, the proposed biosensor is formed in a DG configuration for more electrostatic coupling by the GNRFET device. There are two nanogaps inside both the top and bottom gate oxides to trap the DNA strands. The sensitivity analysis (SA) of the proposed biosensor is computationally performed by solving the Schrödinger Equation (SE) by the non-equilibrium green function (NEGF) method coupled by the Poisson solver (PS), self-consistently. The suggested biosensor gets a high sensitivity to the local environment which is in the result of changing the gate/channel effective coupling owing to the dielectric constant (DC) of inserted DNA.

The framework of the paper is organized as following: The proposed biosensor and operation principle of it is explained in part 2 in details. Part 3 explains the details on the hybridization and forming double-strand DNA structures. A fabrication flow is proposed for realization of the suggested biosensor in the next section. Then an extensive numerical simulation approach for the SA is described in part 5. The other part presents the simulated important results as a result of the hybridization of the DNA biomolecule and also the comparisons with the other reports. Part 7 explains the options can be considered in designing the biosensor (gate length, gate oxide) that impacts the sensitivity of it. The next part makes a discussion on the possible practical challenges which can occur for the biosensor. Finally, the whole paper ends by a comprehensive conclusion in part 9.

2. Proposed DG-AGNRFET biosensor and operation principle

Fig. 1 depicts a perspective of Dual-Gate Armchair-Graphene-Nanoribbon Field-Effect- Transistor abbreviated to the DG-AGNRFET nanostructure. The channel material has been formed by an armchair graphene (A-GNR) by 12 dimmer carbon atoms which is proportional to the width of the device. The physical gate length named as the channel length (L_{ch}) is set to 20 nm. Also, the source/drain extension lengths ($L_{S,D}$) are patterned to the value of 10 nm each. The source/drain regions are doped at the concentration of $2.86 \times 10^8/m$ with no doping on the channel region. Also, the top and bottom gate oxides thickness is defined as 6 nm.

Regarding the graphene layer basic characteristics, the channel material has been realized by an armchair graphene (A-GNR) by 12 dimmer carbon atoms which is proportional to the width of the device. Therefore, the proposed structure utilizes GNR semiconductor as a channel with a width of 0.74 nm which is equivalent to the energy gap of 1.4 eV [31]. Other fundamental parameters in terms of carbon-carbon length, fermi velocity and so on have been presented in [31].

In order to implement the proposed biosensor, the NC is created by a sacrificed layer etching technique started form the end of the source region to the half of the channel region. This cavity or nano-hole which is the place for trapping the biomolecule samples, DNA as a specific biomolecule in this paper, should be electrically detected by the electrostatic modulation.

The biosensor sensitivity (BS) is the result of modification on drain current before and after introducing the DNA biomolecule. Fig. 2 illustrates the important and key part of the biosensor (i.e. NC) exposed to the target DNA. As shown in Fig. 2(a), there is air material inside the NC defined as pre-hybridization step. Regarding the DNA conjugation, hybridized base pairs i.e. Adenine (A) with Thymine (T) and Cytosine (C) with Guanine (G) will form a double-stranded helix texture (dsDNA) showing the hybridization of target DNA inside the NC as shown in Fig. 2(b). The effect of hybridization is measured by the different methods in terms of the change in conductivity of the channel region. Both variations in the drain current and the threshold voltage are considered as the BS parameter in order to detect and quantify the sensing power for the proposed biosensor.

Two different definitions for the important parameter of the BS is given according to Eqs. (1) and (2):

$$TVBS = V_{th-DNA} - V_{th-NoDNA} \tag{1}$$

$$DCBS = \left(\frac{I_{d-NoDNA} - I_{d-DNA}}{I_{d-NoDNA}} \right) \tag{2}$$

In Eq. (1), $V_{th\text{-}DNA}$ is the threshold voltage of the biosensor after introducing the hybridized DNA into the NC and else one is the threshold voltage before the hybridization. The difference between these values is defined as the TVBS. Also, the other parameter in the case of the DCBS giving the relative change in the drain currents before ($I_{d\text{-}NoDNA}$) and after ($I_{d\text{-}DNA}$) which is utilized as sensitivity criterion, too. Throughout the paper, both the parameters in the cases of TVBS and DCBS are computed for the investigation of the EP for the suggested biosensor. It is to note that, the drain current is swiped for the various gate voltages in a specific drain voltage for the situations of before/after hybridization. Then the maximum relative variations of the drain current are evaluated for the swiped gate voltages and finally its maximum value will be selected as the DCBS.

It is important to note that the aim of this paper is not to open the discussions about the different sequences of base pairs of DNAs, but instead the paper models the different dsDNA with a change in the DC of target DNA which is the origin of the electrically modulated detection.

3. DNA hybridization details

This section is attributed to explaining the details of DNA strand structure and hybridization process resulting in forming double-strand DNA inside the NC. As we know the backbone of DNA is based on a

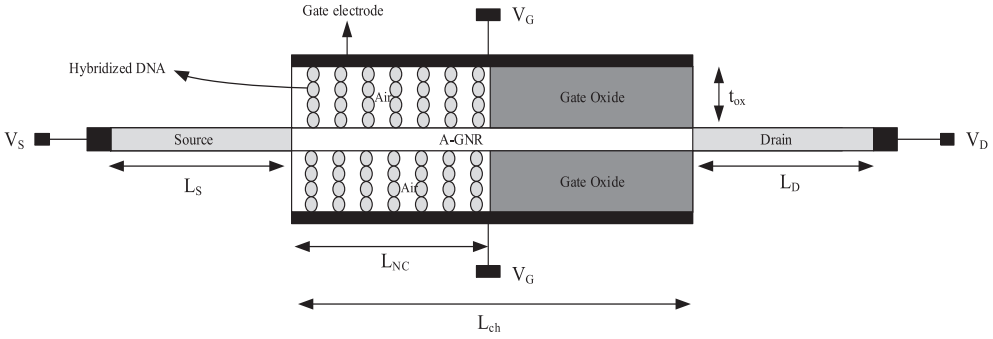

Fig. 1. A cross-sectional view of the proposed biosensor based on the AGNRFET. There are hybridized target DNA inside the nanogap cavity (NC). Nanogap cavity length (L_{NC}) is half of the gate physical length (L_{ch}). Before the hybridization, the DC of the NC is set to $K_{Air} = 1$ and after hybridization will be set to K_{DNA}.

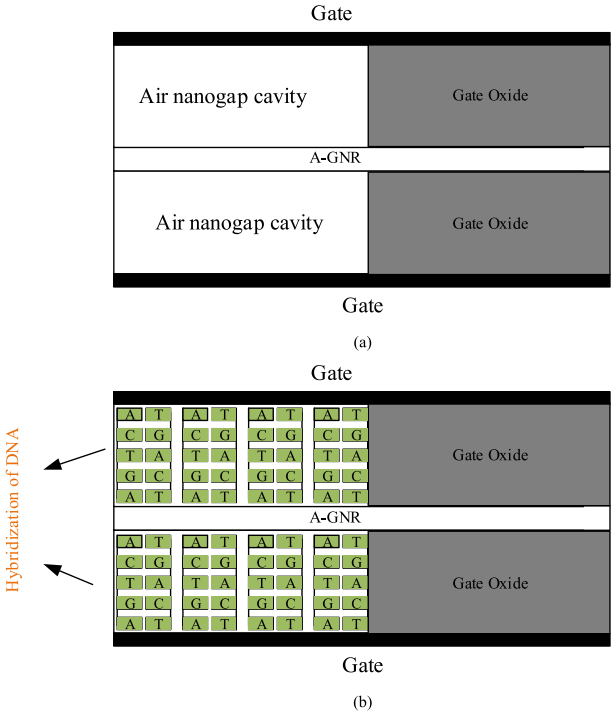

Fig. 2. The DG-AGNRFET biosensor configuration for the SA. (a) before hybridization (In this step whole the NC is only filled by the air) and (b) after hybridization (This step includes the filled NC by the target DNA).

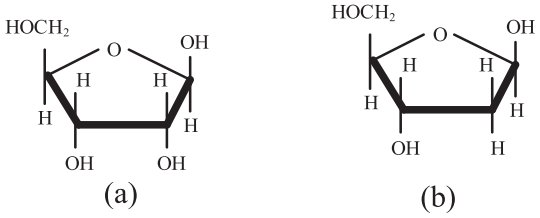

Fig. 3. The structure of (a) Ribose and (b) Deoxyribose. The Deoxyribose is ribose which has lost an oxygen atom.

repeated pattern of a sugar group and a phosphate group. Deoxyribose is a modified form of another sugar called ribose as shown in figure bellow. Ribose is the sugar in the backbone of RNA (ribonucleic acid) as depicted in Fig. 3.

A single-strand DNA is simply a string of nucleotides joined together according to Fig. 4.

The nucleobases can be guanine (G), cytosine (C), thymine (T) and adenine (A) as indicated in the figure by base indicator. Finally, we can now build the chain based on this configuration as illustrated in Fig. 5.

It is a ssDNA which is immobilized inside the NC. The hybridization of the DNA means that an A-T and G-C binding will form when the target DNA is introduced to the NC. Indeed, two strands of DNA will be joint together as shown in Fig. 6. The hybridization of the target DNA will increase the DC of NC resulting in electrostatic modulation of the proposed biosensor. A meaningful result is the successful DNA detection.

It is worth noting that the increase in phosphate group of DNA backbones inside the NC induces a high dielectric constant. As a specific sample, the DNA sequence extracted from *Neisseria gonorrhoeae* [32] can be used for the detection by the proposed biosensor. The probe DNA (pDNA) attached to the surface inside the NC for the hybridization by the target DNA (tDNA) is 5′-thiol-TCGAGCATGAACGTCAGTATTAT-3′. Also, the target DNA sequence is 3′-thiol-AGCTCGTACTTGCAGTCAT AATA-5′. It contains 23-mer base-pair can be easily inserted and fitted inside the NC. The self-assembly monolayer (SAM) technique has been used to immobilize the pDNA in order to attach it onto the tDNA. More details about this procedure has been explained in [32]. After entrance of the solution containing tDNA inside the NC and formation of the hybridization, the nanogap is blow dried by nitrogen. As a result, the DC of the NC implying the DNA dielectric increases [33]. In the result of this action, the effective gate capacitance alters thus modifying the channel conduction of the GNR material will be successfully detected as a result of *Neisseria gonorrhoeae*. It is worth noting that our proposed biosensor is not limited to a specific DNA sequences but each target DNA can be identified since it is basically governed by the permittivity of the hybridized DNA.

4. Fabrication flow of the proposed biosensor

In this section the steps for the fabrication of the proposed biosensor is proposed. The starting stage is forming a graphene layer on the dielectric material by Chemical Vapor Deposition (CVD) technique [34]. Next, by a proper cutting, the graphene nanoribbon will be made according to [35]. Fig. 7 (a) shows the conventional process including making gate oxide, source/drain regions performed by the photolithography, ion implantation and wet etching according to [36,37]. In the figure, the procedures which are required has been indicated. Afterward, the gate electrode is deposited as shown in Fig. 7(b). Fig. 7(c) shows the stage related to the creation of the NC. The lateral wet etching has been utilized to make the NC. The nanogap length is controlled by duration of lateral wet etching with diluted buffered oxide etchant (BOE) [38]. It is noted that the gate oxide is utilized as a sacrificed layer in order to leave the NC [5,38]. The SAM method is used to immobilize the DNA probes on a solid surface [38]. Finally, the source and drain contacts can be created according to the processes used for a conventional MOSFET as shown in Fig. 7(d).

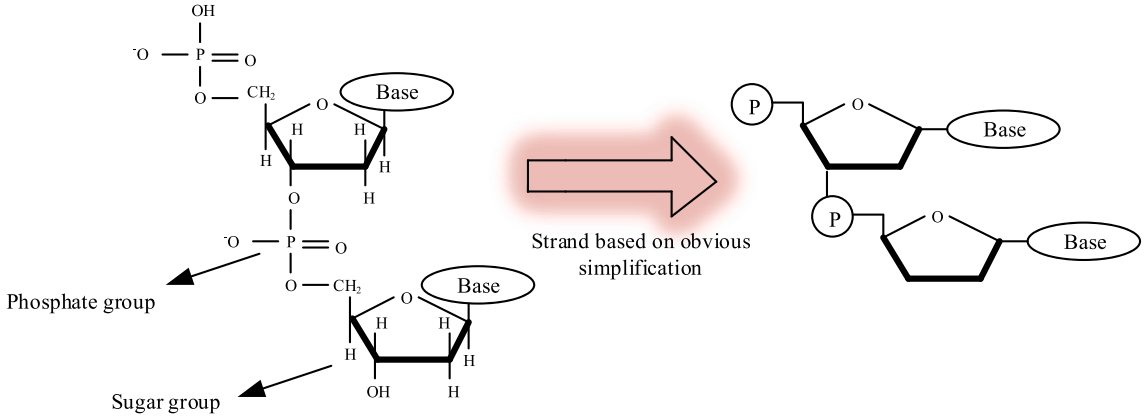

Fig. 4. A view of DNA chain in left-hand. Right-hand illustration is the chain based on obvious simplification.

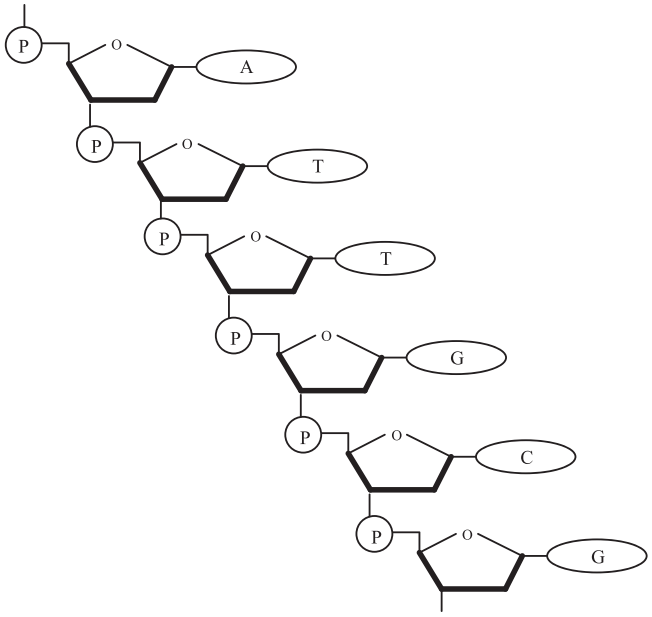

Fig. 5. A complete chain of DNA including 6 nucleobases.

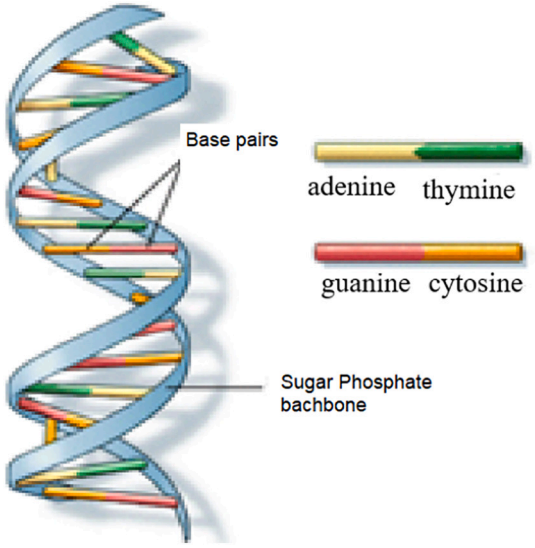

Fig. 6. The formation of double-strand DNA after hybridization.

5. Numerical simulation approach

As previously stated, the NEGF formalism which is the most precise approach for the simulation of nanostructures is utilized to model the carrier transport in the proposed biosensor. This method is commonly used to find the energy levels contributed to the channel conduction. Indeed, the SE is solved by the NEGF coupled by the PS, self-consistently. The algorithm starts with an initial guess on the potential profile which is usually zero. Then the energy level of the channel region is extracted by the NEGF method, thus the amount of net charge inside the channel region can be computed. Afterward, this computed charge goes to the PS to find the new potential profile. The algorithm will continue until the absolute difference between the successive potential profiles will be less than 1 meV. Regarding the parameters in terms of the energy levels, the net charge density the potential profile, and the drain current is evaluated by the transfer matrix method. The procedure for the convergence of the simulation approach is illustrated in Fig. 8.

With performing a chain of mathematical computations and assumptions, we are directed the real space (RS) to the mode space (MS) in order to improve the computational efficiency reducing computed cost and time-consuming issues [39]. To more clarify the methodology, Fig. 9 presents a view of the atomistic structure for the channel region of the proposed biosensor. As shown in the figure, the channel region is made by 12 dimmer carbons which is proportional to the GNR width. Two sub-lattices P1 and P2 are repeated to form the GNRFET. In the MS method, the structure is divided into many one-dimensional chains that each is named as mode g [39]. With the help of the transform matrix, the Hamiltonian of the structure in the RS is converted to that in the MS. Actually, we now have a Hamiltonian matrix for each mode g. It is to note that these modes are completely decoupled from each other. The nearest neighboring approximation for the Hamiltonian has been considered to model the atomistic structure of the suggested biosensor. The source/drain Fermi energy level (E_{FS}/E_{FD}), biosensor Hamiltonian (H_g) and source/drain self-energies Σ_S/Σ_D are clearly observed in the figure.

The simulation approach starts with the computation of the Retarded Green Function (RGF) according to the subsequent form:

$$G_E = \left[(E + i\varepsilon^{+})I - H_g - \sum\nolimits_S - \sum\nolimits_D\right]^{-1} \quad (3)$$

In the equation above, E is the energy level, G_E is the RGF, ε is a very small positive quantity, H_g is the Hamiltonian for g'th mode, Σ_S and $\Sigma_D$are the self-energies for the source and drain electrodes showing the coupling between the source/drain regions and the channel region, respectively. The Hamiltonian H_g is arranged according to the subsequent form:

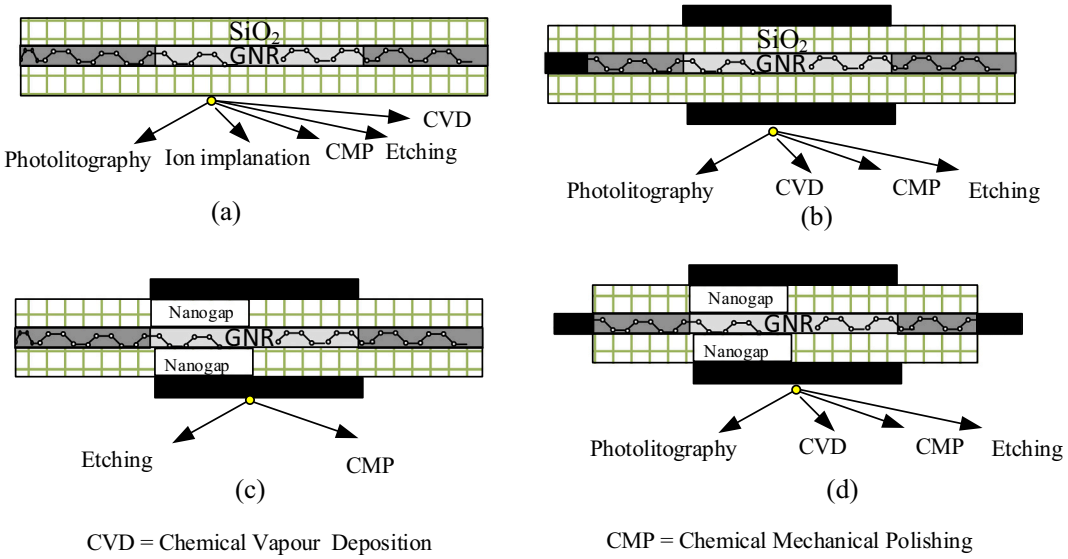

Fig. 7. The procedures for the fabrication of the proposed biosensor.

$$\begin{bmatrix} P_1 & c_{2g} & 0 & \dots \\ c_{2g} & P_2 & c_{1g} & 0 & \cdots \\ 0 & c_{1g} & P_3 & c_{2g} & 0 & \dots \\ 0 & c_{2g} & P_4 & c_{1g} & \dots \\ 0 & c_{1g} & P_5 & \dots \end{bmatrix} \quad (4)$$

It is worth noting that P_m (m = 1,2, …) is the potential in m'th place for g'th mode. The tight-binding parameters c_{1g} and c_{2g} are defined as following:

$$c_{1g} = -2.7eV,\ c_{2g} = 2c_{1g}\cos\left(\frac{g\pi}{n+1}\right) \quad (5)$$

There is a simplified analytical form for the evaluation of the self-energies given as the subsequent relation:

$$\sum_{Sg(Dg)} = \frac{(E - P_{S(D)})^2 + c_{1g}^2 - c_{2g}^2 + \sqrt{(E - P_{S(D)})^2 + c_{1g}^2 - c_{2g}^2 - 4(E - P_{S(D)})^2 c_{1g}^2}}{2(E - P_{S(D)})} \quad (6)$$

where $P_{S(D)}$ is the potential at the interface of the source/drain electrodes and the channel region.

Resolved local density of states (RLDOS) defining the coupling between the source/drain electrodes and the channel region is given as the subsequent form:

$$DOS_{S(D)} = G_E.\, i\left(\sum_{S(D)} - \sum^{\dagger}_{S(D)}\right).\, G_E^{\dagger} \quad (7)$$

In the equation above, the energy level broadening and the RGF have the main role to compute the RLDOS. Regarding to the RLDOS, the net charge density can be computed as follow:

$$Ch\arg e = \int dE\,\mathrm{sgn}(E - E_{Ne})\left\{DOS_S(E) f\left(\mathrm{sgn}(E - E_{Ne})(E - E_{FS}) + DOS_D(E) f\left(\mathrm{sgn}(E - E_{Ne})(E - E_{FD})\right)\right\}\right. \quad (8)$$

After calculating the net charge density, the charge is inserted in the right-side of the PS to obtain the new potential profile as brought in the equation below:

$$\nabla.\,(\nabla \varepsilon P) = -q.\, Ch\arg e \quad (9)$$

The most important quantity in the equation above is the local DC, ε. In the proposed biosensor, this value is 1 before the introduction of the DNA to the NC and is K_{DNA} for after the hybridization of target DNA inside the NC. Hence, the electrostatic of the channel region will be modified by changing the conductivity of the biosensor. For measuring this modification, the drain current should be computed according to Landauer-Buttiker formalism (after getting the convergence of the computational algorithm as illustrated in Fig. 8) given as following:

$$I = \frac{2q}{h}\int TM(E)[f(E - E_{FS}) - f(E - E_{FD})]\,dE \quad (10)$$

The variables in the cases of q and h indicate the electron charge and Plank constant, respectively. Also, TM(E) equals to $Tr\left(i\left(\sum_S - \sum^{\dagger}_{S)}\right)G_E i(\sum_D - \sum^{\dagger}_{D})G_E^{\dagger}\right)$ which Tr is trace operator.

6. Label-free detection of DNA by suggested biosensor

This section is attributed to giving vital information about the parameter of SA of the suggested biosensor i.e. DG-AGNRFET with an NC setup. The change in electrostatic of the channel region is caused by the introduction of the target DNA to the NC. The detection of the DNA biomolecule will be performed when the drain and gate voltages are

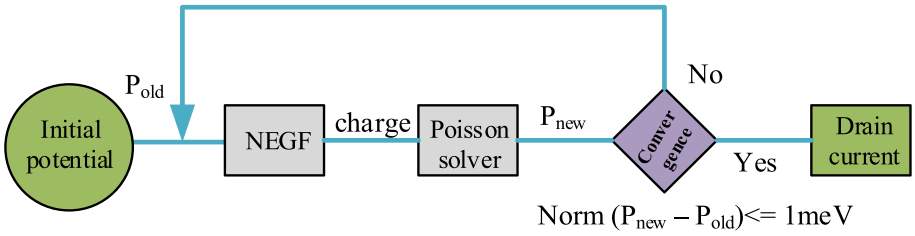

Fig. 8. The flowchart for the numerical simulation approach utilized in the biosensor.

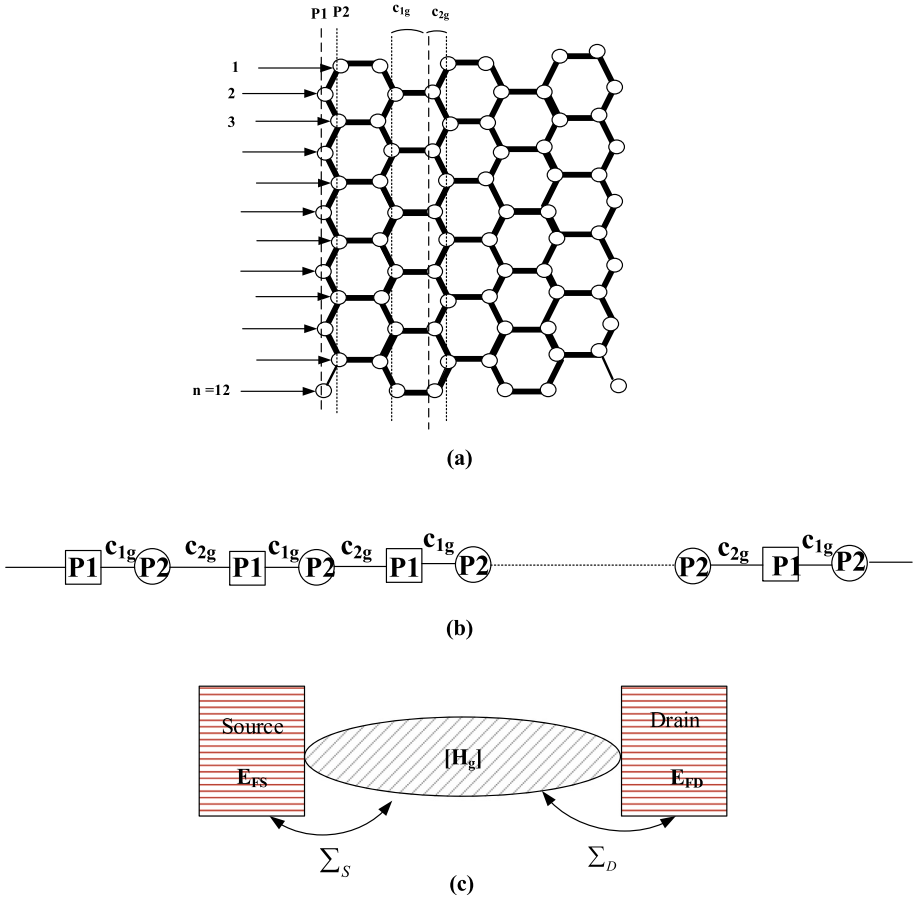

Fig. 9. (a) A view of the atomistic structure of the AGNRFET with 12 dimmer carbon atoms and sub-lattices P1 and P2. (b) The structure in the real space is converted into one-dimensional chains in the mode space (mode g). (c) the formalism of NEGF computing the carrier transport throughout the channel region.

applied. Measuring the resultant drain current computed according to Eq. (10), the SA will be calculated according to Eqs. (1) and (2). Also, the various samples of the target DNA showing the different base pairs sequences can be modeled. The various values of the DC of the biomolecule (K_{DNA} = 2.1, 4, 8, 16, and 32) are investigated. Actually, the DC of the DNA samples depends on the dsDNA density inside the NC. A DNA sequence extracted from *Neisseria gonorrhoeae* (as explained in pervious paragraphs) is considered as a special case for the evaluation of the biosensor in following. It is worth noting that the sensing performance is not limited to this sample but every target DNA can be identified by the proposed biosensor. In order to show the usable detection region for the proposed biosensor the target DNA has been assumed by the different DC.

To have a deep understanding, the conduction band energy (CBE) along the longitudinal direction on the GNR surface is plotted in Fig. 10**.** It is clear from the figure that the CBE will experience a different profile for the target DNA by the different DC. The reason is related to the change in the effective gate capacitance when the DC of the NC varies. Hence, NC setup inside the gate oxides of the DG-GNRFET biosensor can be an attractive approach.

There are some parameters used to perform the SA on the biosensor. The drain current is one of these important parameters commonly involved in the detection and identification of target DNAs. Fig. 11 gives the information about the drain current of the suggested biosensor. The drain current data is shown as a function of the drain voltage for the different gate voltages.

In this step, the typical target DNA is supposed to have a DC by K_{DNA} = 2.1 for the case study. As illustrated in the figure, the drain current will vary when the hybridization of DNA occurs inside the NC.

To better clarify the SA of the suggested biosensor, Fig. 12

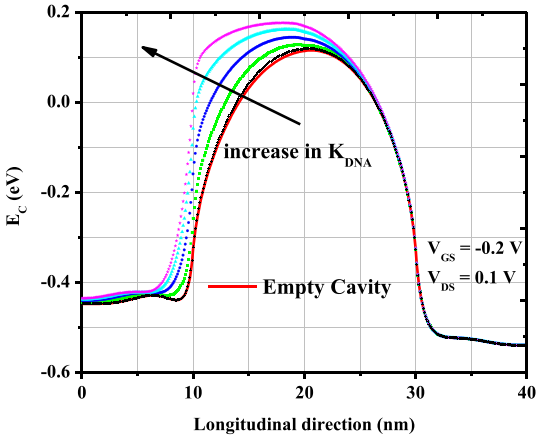

Fig. 10. The CBE profile along the lateral direction of the AGNRFET biosensor. The different DC of target DNA with the K_{DNA} = 2.1, 4, 8, 16 and 32 have been introduced to the NC.

demonstrates the drain current against the gate voltage at the applied bias V_{DS} = 1 V. According to the figure, before the DNA hybridization, the NC is filled by the air leads to reducing the total effective capacitance. One meaningful result is that the minimum value of the drain current will be obtained in this situation. The figure reveals that the drain current is modified when the DNA is introduced to NC. The interesting point is that this modification is explored for both the subthreshold and above the threshold (ON region).

The transmission as one of the main and fundamental parameters

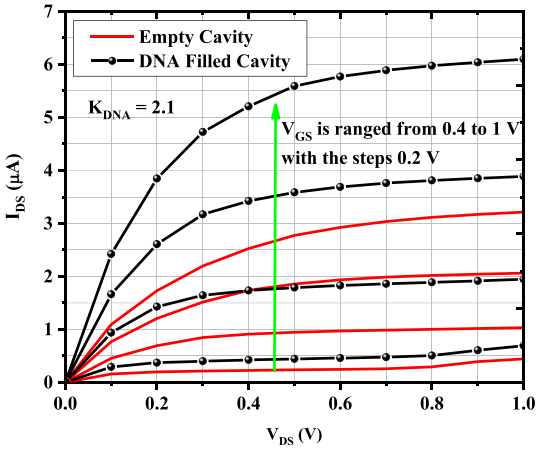

Fig. 11. Drain current as a function of the drain voltage for the different gate voltages. The target DNA with the DC of 2.1 is supposed in this case.

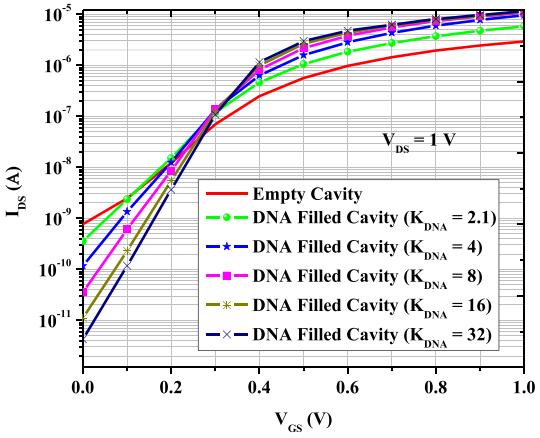

Fig. 12. Drain Current as a function of the gate voltage.

which is directly impacting on the conduction of the channel region has been demonstrated in Fig. 13 for the target DNA with K_{DNA} = 2.1 as a case study. That shows the transmission (TM(E) at Eq. (10)) of the proposed biosensor after the hybridization gets higher than that before hybridization which is made the structure sensitive to the attached DNA biomolecule. Hence, NC setup inside the gate oxides can be taken into account as a useful technique that electrically detect the DNA biomolecule without any labeling process.

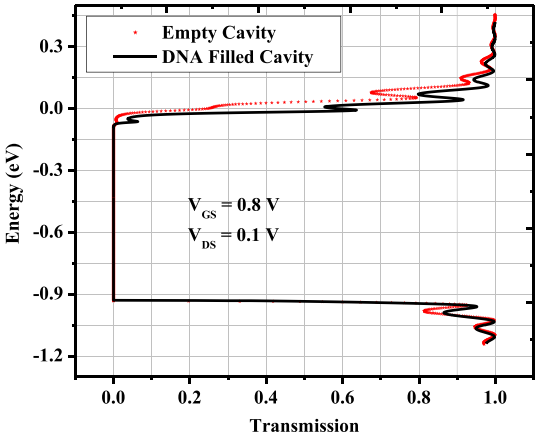

Fig. 13. Transmission curve dependent on the energy level of the AGNRFET before and after the hybridization of the DNA.

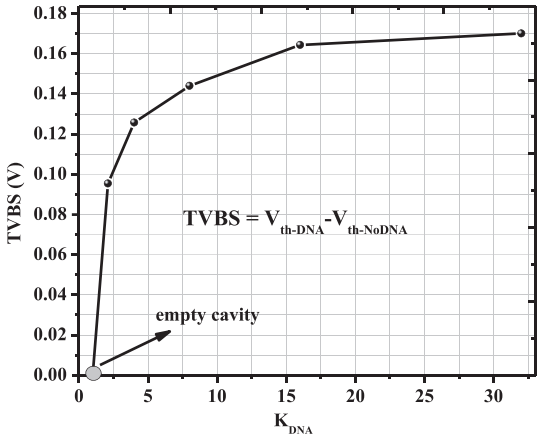

Fig. 14. The SA in the case of the TVBS versus K_{DNA}.

It is the time to perform a SA on the suggested biosensor for the aims of the detection. At first, the BS based on the threshold voltage (the variable TVBS at Eq. (1)) is evaluated. The parameter of TVBS mentions the difference between the threshold voltage before and after hybridization of the target DNA. In order to define the threshold voltage, the fixed current method is utilized for the analysis. Fig. 14 depicts the TVBS as a function of K_{DNA}. This value is zero for empty NC, so this situation is a reference when the target DNA is introduced. The figure shows the TVBS increases when K_{DNA} raises which is very desirable. Also, there is a sudden increase in the TVBS when K_{DNA} is starting to raise. The high value of TVBS will promise an excellent biosensor for the detection. In addition, since the slope of the TVBS curve is high with respect to K_{DNA}, so a wide usable detection region will be realized for the proposed biosensor which is very efficient and useful. Moreover, it is seen a saturation for high K_{DNA} on the curve limited the identification capability for the high concentration of target DNA biomolecules which is known to exist for all the biosensors.

By and large the NC setup inside the gate oxides of the proposed biosensor gives an ability to detect and identify the DNA samples, successfully.

We have introduced the other figure of merit in order to execute the SA. For this reason, the relative variation rate of drain current has been measured given in Eq. (2) before and after hybridization of DNA. At first, the drain current is evaluated against the gate voltage for the NC filled by air (pre-hybridization). Considering a specific target DNA, the drain current is then extracted. Now, these drain current data are applied to the Eq. (2) and finally its maximum is attributed to the DCBS. Fig. 15 illustrates our effort for quantifying the DCBS. It is clearly observed from the plot that the biosensor gets a high DCBS for the DNA by distinct DCs. Further, the high slope of the DCBS will declare a good identification for them. Comparing the parameters in the cases of the DCBS and TVBS together, they will grant interesting information about the identification of the DNA. As shown in Figs. 14 and 15, the DCBS gives only a high identification rate for small K_{DNA} whereas the TVBS keeps the high identification for more kinds of DNA. As a meaningful exploration, the criterion of DCBS is very suitable for identification of the DNAs with the small DC, because its slope gets a very high value as compared to that of the TVBS. For the DNA biomolecules with the moderate and large DC, the TVBS is proposed for identification. In spite of this competition between two main parameters, there is an important similarity. That is the excellent detection of target DNA when it is inserted and hybridized inside the NC.

Regarding the presented results, for highlighting the considerable advance of this work in detecting the biomolecules, comparison between the proposed biosensor and previously published reports has been done and listed at Table 1. In all these reports the criterion of the threshold voltage variation (TVBS) has been considered for measuring

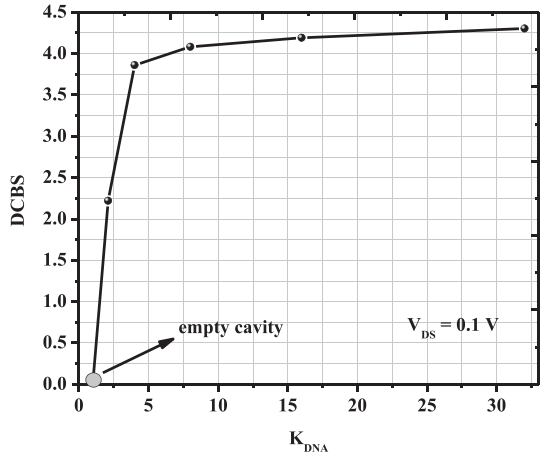

Fig. 15. The SA in the case of the DCBS versus K_{DNA}.

Table 1
The comparison between proposed biosensors and other reports.

Parameters biosensor		Area filled by the biomolecule (nm_j^2)	TVBS/ $area_{nanogap}$ (mV/nm^2)	Total effective area of device (nm^2)
This work		120	1	240
Reports	[38]	2.5e3	0.008	4.5e9
	[32]	7.5e3	0.26	78e3
	[22]	5e3	0.01	3.5e9
	[7]	1.5e3	3	23e3
	[40]	12e3	0.004	65e3
	[41]	300	0.33	4e3

the sensitivity. In order to perform a fair comparison, the area of NC filled by the biomolecules ($Area_{nanogap}$) must be considered.

Hence, the relative sensing performance metric computed as $\frac{TVBS}{Area_{nanogap}}$ is introduced to quantify the power of detection [42]. This performance metric can be defined as relative sensitivity. It is evident that its high value is very advisable and promising. As the table illustrates, the proposed structure gets a good detection by having a very high RS (1 mV/nm^2). The situation will be more interesting when we see that the minimum area covered by the biomolecule is related to the proposed biosensor (120 nm^2) which is showing the marvelous importance of the proposed biosensor. Also, the total effective device area of the biosensors has been given in the table. It is interesting to know that the proposed biosensor grants another advantage. It is given the least effective device area around 240 nm^2 which is very low in comparison with its counterparts. Although, the report based on [7] has given a more RS but it is important to consider both covered area by the biomolecule and also the total effective device area which is much more than those in the proposed biosensor. Also, the conduction mechanism in the biosensor based on [7] is severely governed by the impact ionization needing a high applied biases on the electrodes whereas the proposed biosensor requires a small bias and also its sensing performance will be enhanced even for scaled gate lengths. Hence, the proposal of utilizing GNRFET as a biosensor according to this work is very interesting and can verified as an efficient, highly sensitive and ultra-scale biosensor.

7. Discussion on designing issues

This section will perform a study on designing options. We decided to provide a useful guideline in order to utilize the DG-AGNRFET biosensor for the DNA detection and identification by high efficiency. At first, the effect of L_{ch} on the sensitivity of the biosensor is carefully monitored. Three different L_{ch} (10 nm, 15 nm and 20 nm) are selected

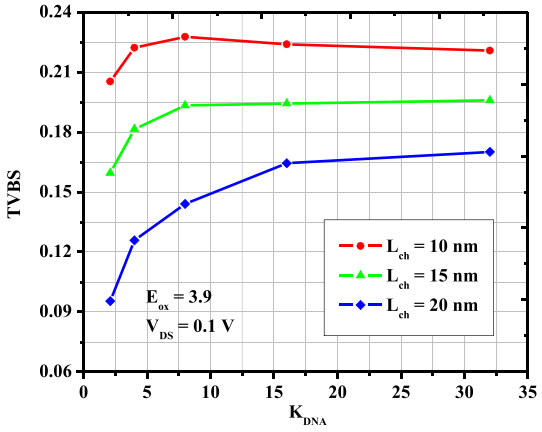

Fig. 16. The TVBS against K_{DNA} for the different L_{ch}.

for the performance comparison. Fig. 16 illustrates the TVBS parameter for the distinct DC target DNA. There is a marvelous exploration from this figure for the proposed biosensor. An increase in the values of TVBS is seen when the channel length is scaled down. Considering this increase, it is concluded that the suggested biosensor is a very attractive candidate for ultra-scale aims. Indeed, the SCEs will help the DG-AGNRFET biosensor to successfully detect the DNA biomolecules by increase in sensitivity which is very favorable.

One of the main parameters that can impact the sensitivity of the biosensor is the gate oxide material. Till now, the SiO_2 has been utilized as the gate oxide. In order to investigate its role, the DCBS contour showing the sensitivity for the different gate oxides and target DNA depicted in Fig. 17. It will give us information that the sensitivity gets the highest for the gate oxides with the DC of greater than 17 and K_{DNA} more than 15. This figure also tells us which the DNA concentration and which the gate oxide can be led to a specific detection level. The difference between the highest sensitivity and the least sensitivity for a specific gate oxide can be illustrative of the identification of the target DNA. As can be interpreted from the figure, the more increase the gate oxide DC, the more sensitivity will be explored. This can cause that we get a good framework for designing of the DG-AGNRFET biosensor.

8. Discussion on possible practical challenges

In this section a brief discussion is performed on the practical issues which can impact on the sensing performance. It is worth noting that

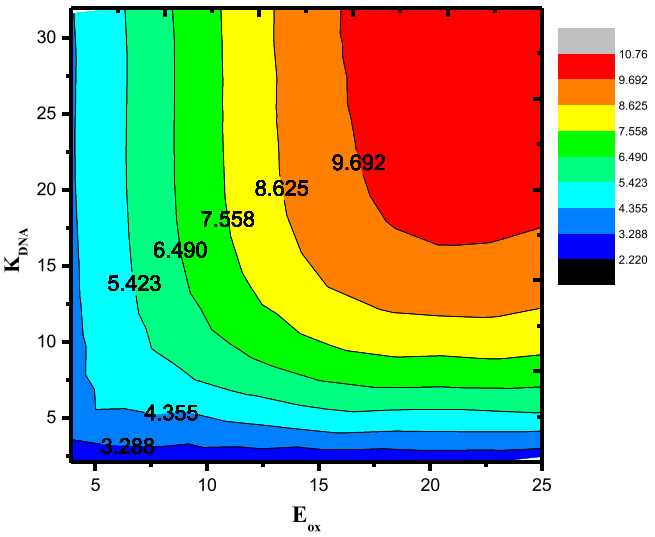

Fig. 17. The DCBS contours versus K_{DNA} and E_{ox}.

these issues are seen for all biosensor in the real conditions. This work presents a novel dielectrically modulated TFET based biosensor through an extensive simulation approach. The active channel of the biosensor is made by the graphene nanoribbon in a double-gate configuration. We benefited from the NC technology inside the gate oxide to trap the biomolecules (target DNA in this specific case). As we know there are some devices in the basis of enzyme, fluorescent, electromagnetic and ISFET to detect the biomolecules. All of these devices have been known by giving a low selectivity. But, after exploring the NC concept this concern has been reduced due to the detection mechanism occurs inside a NC which is free of any solation. For example, the gate electrode in the ISFET is assumed to be a solution. This solution can seriously impact on the selectivity, linear detection range, detection limit and also the sensitivity. But the scenario is very different in a NC technology-based biosensor. Actually, there is a solid-state gate electrode on the top of the channel and the NC.

One of the important issues in evaluation of the fabricated biosensors is about the selectivity. Proposal of the efficient techniques for the immobilization of DNA probes can increase the selectivity. There are a few approaches to immobilize the DNA probe inside the NC. The SAM method is commonly used to immobilize the DNA probes on a solid surface [4,32,38]. Although, this technique is widely used but it needs an extra action to enhance the surface efficiency such as including oxygen plasma and a heating annealing resulting in a getting a biosensor by high selectivity. Also, a new method has been reported to immobilize the biomolecule probes using silica-binding proteins (SBP) which has a strong binding with the SiO_2 surface [43]. It has been proved that this new method presents a very high selectivity for the biosensors in comparative to the SAM method.

One of the other issues can degrade the sensing performance of the proposed biosensor like other biosensors, is related to the partial hybridization that may occurring inside the NC. Throughout the paper, it has been assumed that the target DNA is completely filled inside the NC for the simplicity. Moreover, one of the problems is that the biomolecule can be partially distributed inside the NC resulting in decreases the sensitivity performance [23] . Also, the positions of DNA discrete entity probes can be defined as the other parameter to impact on the sensitivity. All these effects can be analytically modeled for the proposed biosensor like those reported in [23].

The single-base mismatches of DNA and non-complementary DNA are the important factors can degrade the sensing performance. In order to solve the concerns for these issues for the proposed biosensor, we can benefit from Peptide Nucleic Acid (PNA) probes. It has been proved the PNA probes are very suitable and promising for sequence-specific DNA biosensors by a potent and excellent capability in the discrimination of the single-base mismatches of DNA [44]. Also, these probes are known to be insensitive to non-complementary DNA [44]. Hence, these probes can be a suitable replacement for the single-strand DNA probes getting a high efficiency in the detection.

9. Conclusion

For the first time, an NC setup as an entrance of the target DNA biomolecules has been embedded in the DG-AGNRFET structure benefiting from the armchair graphene as the channel region for the detection. When the samples of DNA are hybridized in the NC, the electrostatic of the channel region made form armchair graphene by the index of 12 will be modified led to increasing the channel transmission. The DG-AGNRFET biosensor has been simulated with the NEGF technique coupled by the PS, self-consistently. Both definition of the SA in terms of the TVBS and DCBS revealed high detection of the proposed biosensor for the target DNA. Also, the proposed biosensor has given a wide usable detection region which is very desirable. Moreover, the paper states that the TVBS method is more efficient than the DCBS method in the recognition of the DNA biomolecule. The results revealed a relative sensitivity of 1 mV/nm^2 by a filled area and the DNA about 120 nm^2 showing the excellent superiority for the proposed biosensor as compared to other counterparts. The effective area of the proposed biosensor obtains 240 nm^2 which is very small in comparison with other reports highlighting the great capability of the biosensor in the ultra-scale detection applications. Also, a detailed discussion on the designing issues showed that scaling down of the device will increase the detection power of the proposed biosensor that is very important and promising. All the obtained outcomes introduce the DG-AGNRFET structure as an efficient biosensor with high detection and identification power of the tDNA that can be taken as a powerful candidate for ultra-scale, low-cost and label-free bio-sensing applications.

Declaration of competing interest

The authors have no conflict of interest.

References

[1] H. Karimi-Maleh, F. Karimi, M. Alizadeh, A.L. Sanati, Electrochemical sensors, a bright future in the fabrication of portable kits in analytical systems, Chem. Rec. (2020), https://doi.org/10.1002/tcr.201900092.

[2] A. Khodadadi, E. Faghih-Mirzaei, H. Karimi-Maleh, A. Abbaspourrad, S. Agarwal, V.K. Gupta, A new epirubicin biosensor based on amplifying DNA interactions with polypyrrole and nitrogen-doped reduced graphene: experimental and docking theoretical investigations, Sensors Actuators B Chem. 284 (2019) 568–574.

[3] J. Mohanraj, D. Durgalakshmi, R.A. Rakkesh, S. Balakumar, S. Rajendran, H. Karimi-Maleh, Facile synthesis of paper based graphene electrodes for point of care devices: a double stranded DNA (dsDNA) biosensor, J. Colloid Interface Sci. 566 (2020) 463–472.

[4] A. Poghossian, A. Cherstvy, S. Ingebrandt, A. Offenhäusser, M.J. Schöning, Possibilities and limitations of label-free detection of DNA hybridization with field-effect-based devices, Sensors Actuators B Chem. 111 (2005) 470–480.

[5] H. Im, X.-J. Huang, B. Gu, and Y.-K. Choi, "A dielectric-modulated field-effect transistor for biosensing," *Nature nanotechnology,* vol. 2, no. 7, p. 430, 2007.

[6] M. Im, J.-H. Ahn, J.-W. Han, T.J. Park, S.Y. Lee, Y.-K. Choi, Development of a point-of-care testing platform with a nanogap-embedded separated double-gate field effect transistor array and its readout system for detection of avian influenza, IEEE Sensors J. 11 (2) (2010) 351–360.

[7] N. Kannan, M.J. Kumar, Dielectric-modulated impact-ionization MOS transistor as a label-free biosensor, IEEE electron device letters 34 (12) (2013) 1575–1577.

[8] D.M. Wilson, S. Hoyt, J. Janata, K. Booksh, L. Obando, Chemical sensors for portable, handheld field instruments, IEEE Sensors J. 1 (4) (2001) 256–274.

[9] J. Wu, et al., DNA-stabilized silver nanoclusters for label-free fluorescence imaging of cell surface glycans and fluorescence guided photothermal therapy, Anal. Chem. 90 (24) (2018) 14368–14375.

[10] Y. Yao, et al., DNA-templated silver nanocluster/porphyrin/MnO2 platform for label-free intracellular Zn2+ imaging and fluorescence-/magnetic resonance imaging-guided photodynamic therapy, ACS Appl. Mater. Interfaces 11 (15) (2019) 13991–14003.

[11] Y. Yao, et al., Multifunctional Fe3O4@ polydopamine@ DNA-fueled molecular machine for magnetically targeted intracellular Zn2+ imaging and fluorescence/MRI guided photodynamic-photothermal therapy, Anal. Chem. 91 (12) (2019) 7850–7857.

[12] H. Karimi-Maleh, A. Bananezhad, M.R. Ganjali, P. Norouzi, A. Sadrnia, Surface amplification of pencil graphite electrode with polypyrrole and reduced graphene oxide for fabrication of a guanine/adenine DNA based electrochemical biosensors for determination of didanosine anticancer drug, Appl. Surf. Sci. 441 (2018) 55–60.

[13] S.C. Jakeway, A.J. de Mello, E.L. Russell, Miniaturized total analysis systems for biological analysis, Fresenius J. Anal. Chem. 366 (6–7) (2000) 525–539.

[14] M.K. Anvarifard, A.A. Otttttttrji, Evidence for enhanced reliability in a novel Nanoscale partially-depleted SOI MOSFET, IEEE Trans. Device Mater. Reliab. 15 (4) (2014) 536–542.

[15] M.K. Anvarifard, Z. Ramezani, I.S. Amiri, A.M. Nejad, A nanoscale-modified band energy junctionless transistor with considerable progress on the electrical and frequency issue, Mater. Sci. Semicond. Process. 107 (2020) 104849.

[16] M. Karbalaei, D. Dideban, A nanoscale silicon on insulator transistor with superior performance using dual material gate and retrograde/halo doping in source/drain sides, J. Phys. Chem. Solids 138 (2020) 109247.

[17] S.J. Mahabadi, S. Rajabi, J. Loiacono, A novel partial SOI LDMOSFET with periodic buried oxide for breakdown voltage and self heating effect enhancement, Superlattice. Microst. 85 (2015) 872–879.

[18] A. Naderi, F. Heirani, Improvement in the performance of SOI-MESFETs by T-shaped oxide part at channel region: DC and RF characteristics, Superlattice. Microst. 111 (2017) 1022–1033.

[19] Z. Ramezani, A.A. Orouji, S.A. Ghoreishi, I. Amiri, A nano junctionless double-gate MOSFET by using the charge plasma concept to improve short-channel effects and frequency characteristics, J. Electron. Mater. 48 (11) (2019) 7487–7494.

[20] Z. Ramezani, A.A. Orouji, Investigation of veritcal graded channel doping in nanoscale fully-depleted SOI-MOSFET, Superlattice. Microst. 98 (2016) 359–370.

[21] Z. Ramezani, A.A. Orouji, A novel double gate MOSFET by symmetrical insulator

packets with improved short channel effects, Int. J. Electron. 105 (3) (2018) 361–374.
[22] C.-H. Kim, J.-H. Ahn, K.-B. Lee, C. Jung, H.G. Park, Y.-K. Choi, A new sensing metric to reduce data fluctuations in a nanogap-embedded field-effect transistor biosensor, IEEE transactions on electron devices 59 (10) (2012) 2825–2831.
[23] R. Narang, M. Saxena, M. Gupta, Comparative analysis of dielectric-modulated FET and TFET-based biosensor, IEEE Trans. Nanotechnol. 14 (3) (2015) 427–435.
[24] M. K. Anvarifard, Z. Ramezani, and I. S. Amiri, "Proposal of an Embedded Nanogap Biosensor by a Graphene Nanoribbon Field-Effect Transistor for Biological Samples Detection," *physica status solidi (a),* vol. 217, no. 2, p. 1900879, 2020.
[25] J. Ji, et al., Simultaneous noncovalent modification and exfoliation of 2D carbon nitride for enhanced electrochemiluminescent biosensing, J. Am. Chem. Soc. 139 (34) (2017) 11698–11701.
[26] M. K. Anvarifard, "Modeling a Double-Halo-Doping Carbon Nanotube FET in DC and AC Operations," *ECS Journal of Solid State Science and Technology,* vol. 7, no. 12, p. M209, 2018.
[27] M.A. Eshkalak, M.K. Anvarifard, A guideline for achieving the best electrical performance with strategy of halo in graphene nanoribbon field effect transistor, ECS Journal of Solid State Science and Technology 5 (12) (2016) M141–M147.
[28] M.A. Eshkalak, M.K. Anvarifard, A novel graphene nanoribbon FET with an extra peak electric field (EFP-GNRFET) for enhancing the electrical performances, Phys. Lett. A 381 (16) (2017) 1379–1385.
[29] A.Y. Goharrizi, M. Zoghi, M. Saremi, Armchair graphene nanoribbon resonant tunneling diodes using antidote and BN doping, IEEE Transactions on Electron Devices 63 (9) (2016) 3761–3768.
[30] M. Rastgoo, M. Fathipour, Interaction of DNA nucleobases with boron, nitrogen, and sulfur doped graphene nano-ribbon for sequencing: an Ab initio study, Appl. Surf. Sci. 492 (2019) 634–643.
[31] A. C. Neto, F. Guinea, N. M. Peres, K. S. Novoselov, and A. K. Geim, "The electronic properties of graphene," *Reviews of modern physics,* vol. 81, no. 1, p. 109, 2009.
[32] C.-H. Kim, C. Jung, H.G. Park, Y.-K. Choi, Novel dielectric modulated field-effect transistor for label-free DNA detection, Biochip J 2 (2) (2008) 127–134.
[33] A. Cuervo, P.D. Dans, J.L. Carrascosa, M. Orozco, G. Gomila, L. Fumagalli, Direct measurement of the dielectric polarization properties of DNA, Proc. Natl. Acad. Sci. 111 (35) (2014) E3624–E3630.
[34] Y. Iyechika, "Application of Graphene to High-speed Transistors: Expectations and Challenges," Citeseer1349-3663, (2010).
[35] K. Mohanram and J. Guo, "Graphene nanoribbon FETs: Technology exploration and CAD," in *2008 IEEE/ACM International Conference on Computer-Aided Design*, 2008, pp. 412–415: IEEE.
[36] J.-H. Ahn, S.-J. Choi, J.-W. Han, T.J. Park, S.Y. Lee, Y.-K. Choi, Double-gate nanowire field effect transistor for a biosensor, Nano Lett. 10 (8) (2010) 2934–2938.
[37] L. Rispal and U. Schwalke, "Structural and electrical characterization of carbon nanotube field-effect transistors fabricated by novel self-aligned growth method," in *2008 3rd International Conference on Design and Technology of Integrated Systems in Nanoscale Era*, 2008, pp. 1–5: IEEE.
[38] C.-H. Kim, C. Jung, K.-B. Lee, H. G. Park, and Y.-K. Choi, "Label-free DNA detection with a nanogap embedded complementary metal oxide semiconductor," *Nanotechnology,* vol. 22, no. 13, p. 135502, 2011.
[39] P. Zhao and J. Guo, "Modeling edge effects in graphene nanoribbon field-effect transistors with real and mode space methods," *Journal of Applied Physics,* vol. 105, no. 3, p. 034503, 2009.
[40] J.-M. Choi, J.-W. Han, S.-J. Choi, Y.-K. Choi, Analytical modeling of a nanogap-embedded FET for application as a biosensor, IEEE transactions on electron devices 57 (12) (2010) 3477–3484.
[41] S. Kanungo, S. Chattopadhyay, P.S. Gupta, K. Sinha, H. Rahaman, Study and analysis of the effects of SiGe source and pocket-doped channel on sensing performance of dielectrically modulated tunnel FET-based biosensors, IEEE Transactions on Electron Devices 63 (6) (2016) 2589–2596.
[42] M. S. Parihar and A. Kranti, "Enhanced sensitivity of double gate junctionless transistor architecture for biosensing applications," *Nanotechnology,* vol. 26, no. 14, p. 145201, 2015.
[43] B. Gu, T.J. Park, J.H. Ahn, X.J. Huang, S.Y. Lee, Y.K. Choi, Nanogap field-effect transistor biosensors for electrical detection of avian influenza, small 5 (21) (2009) 2407–2412.
[44] J. Wang, et al., Peptide nucleic acid probes for sequence-specific DNA biosensors, J. Am. Chem. Soc. 118 (33) (1996) 7667–7670.